Case Reports in Oncology

Case Rep Oncol 2022;15:413–422
DOI: 10.1159/000523896
Received: January 31, 2022
Accepted: February 24, 2022
Published online: April 21, 2022

Case Report

Human Immature Dental Pulp Stem Cells Did Not Graft into a Preexisting Human Lung Adenocarcinoma

Joyce Macedo da Silva[a] Rodrigo Pinheiro Araldi[b, c, d]
Gabriel Avelar Colozza-Gama[d] Eduardo Pagani[a] Ariye Sid[a]
Cristiane Wenceslau Valverde[c] Irina Kerkis[b, d]

[a]Azidus Brazil, São Paulo, Brazil; [b]Genetics Laboratory, Butantan Institute, São Paulo, Brazil; [c]Cellavita Scientific Researches, São Paulo, Brazil; [d]Structural and Functional Biology Post-graduation Program, Federal University of São Paulo (UNIFESP), São Paulo, Brazil

Keywords
Human immature dental pulp stem cell · Huntington's disease · Lung adenocarcinoma · Safety · RNA-sequencing

Abstract
Mesenchymal stem cell (MSC)-based therapies have been considered an attractive approach for treating Huntington's disease (HD). However, due to the pulmonary first-passage effect associated with intravenous infusion (the most commonly used route of MSC administration), there is a rising concern that the cells could be entrapped in the lungs and grafted (homing) into preexisting lung cancer. Herein, we report the case of a patient with HD enrolled in a cell therapy phase I clinical trial for HD treatment having a preexisting pulmonary nodule. The nodule was found at the trial screening. The patient was referred to a pulmonologist who considered the nodule non-cancer and authorized enrollment. The patient received four intravenous administrations of human immature dental pulp stem cells (hIDPSCs) at the dose of 1×10^6 cells/kg of body weight within 2 years. One month after the last dose, a computerized tomography scan showed nodule growth. A bronchoscopy biopsy showed primary lung adenocarcinoma. The neoplasm was surgically excised (lung superior right lobectomy). The patient is cured of the neoplasm. The tumor was sectioned into six fragments, which were subjected to RNA-seq. The transcriptome of each tumor section was compared with the transcriptome of infused hIDPSCs using two statistical approaches: principal component analysis

Joyce Macedo da Silva and Rodrigo Pinheiro Araldi contributed equally.

Correspondence to:
Rodrigo Pinheiro Araldi, rodrigo.pinheiro.araldi@gmail.com
Irina Kerkis, irina.kerkis@butantan.gov.br

Case Rep Oncol 2022;15:413–422
DOI: 10.1159/000523896

and NOIseq. Both results demonstrated a linear distance between the hIDPSCs and the lung adenocarcinoma. These results suggest that the infused hIDPSCs neither home nor graft within the pulmonary nodule.

Introduction

Huntington's disease (HD, OMIM #143100) is an autosomal dominant progressive and incurable neurodegenerative disease caused by an increase of CAG repeats of the huntingtin gene (*HTT locus* 4p16.3), which leads to the progressive death of medium spiny neurons in the striatum [1]. The main goal of cell-based therapies is to repair the mechanisms underlying disease initiation and progression through the trophic effect [2]. Different cell types can be used for this purpose. However, due to its ectomesenchymal origin (neural crest), the human dental pulp stem cells (hDPSCs) exhibit a higher neuroprotective and neurogenic potential when compared to other mesenchymal stem cells (MSCs) [3–5]. For this reason, hDPSCs have been considered for treating neurodegenerative disorders. Studies in 3-nitropropionic HD rat models showed that the intravenous (IV) administration of hDPSCs compensates for the striatal atrophy and downregulates proinflammatory cytokines [4, 5].

The safety of manufactured MSCs for patients with preexisting cancer has been described [6, 7]. However, the transcriptome and phenotype of tissue-resident MSCs ancestors are changed when cultured in vitro (manufactured) and are significantly different from their analogous in vivo [8]. Furthermore, several studies already showed that when recruited to the tumor microenvironment (TME), tissue-resident MSC ancestors can have a pro-tumorigenic phenotype, increasing tumor growth, and eliciting antitumor immune responses, thus supporting successive steps of carcinogenesis [6, 9–11]. These findings raised the question of whether manufactured MSC would mimic the tissue-resident MSC when introduced into the cancer microenvironment.

We developed a novel technology for isolating and expanding human immature dental pulp stem cells (hIDPSCs) with high efficacy [12]. These manufactured cells share their main characteristics with other MSCs [13]. These cells were used in a first-in-human, uncontrolled, open-label, phase I clinical trial with six HD participants (clinicaltrials.gov ID: NCT02728115).

Herein, we describe that the genetic materials from hIDPSCs administered intravenously into a clinical trial participant with preexisting silent pulmonary nodule were not found in a growing lung cancer tissue. Before the pulmonary nodule started to grow, the patient received four IV administrations of hIDPSCs (1×10^6 cells/kg). The first three administrations occurred with a 1-month interval. The fourth administration occurred 2 years later. One month after the last administration, the physician noticed the tumor growth.

Case Presentation

A 51-year-old man with confirmed HD was evaluated for enrollment in a cell therapy phase I clinical trial (https://clinicaltrials.gov/ct2/show/NCT02728115) [14]. He was a heavy smoker for over 20 years and was followed by a pulmonologist. During the trial safety

Case Rep Oncol 2022;15:413–422
DOI: 10.1159/000523896

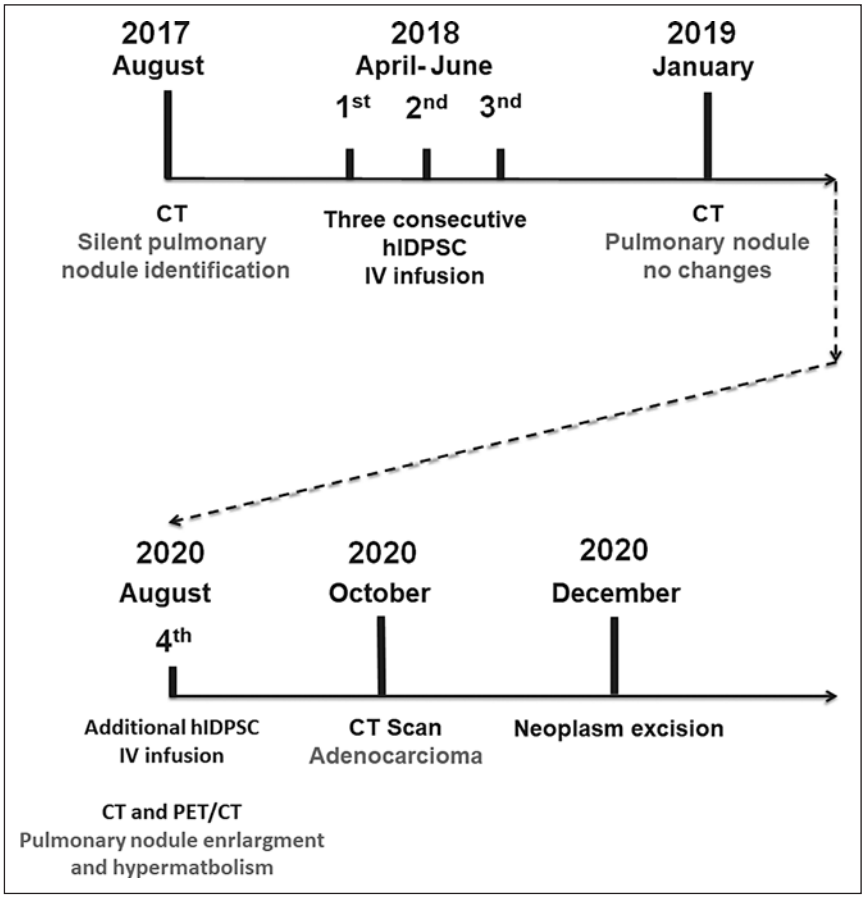

Fig. 1. Time-line of hIDPSC administration in an HD patient with a silent pulmonary nodule following phase 1 clinical protocol and pulmonary lung nodule evolution between December 2017 and December 2020.

assessments, a pulmonary nodule was identified by computerized tomography (CT)scan (August 16, 2017 dimensions 13 × 15 × 17 mm). His pulmonologist opined that the nodule was probably non-cancer, and balancing the risks and benefits for his severe HD, authorized the enrollment.

The patient received 3 monthly IV administrations of hIDPSCs (which correspond to the investigational product NestaCell®), using the cell dose of 10^6 cells/Kg weight (Fig. 1): April 3, 2018, May 8, 2018, June 5, 2018. The participant remained hospitalized after administration for approximately 48 h in an intensive care unit and was discharged. The participant underwent a new medical evaluation after 15 days and 30 days and was released for outpatient follow-up and returns as described in the protocol.

The investigational product NestaCell™ was manufactured according to the good manufacturing practices in the Cellavita facility (Valinhos, Brazil). The hIDPSCs were isolated from the dental pulp of deciduous teeth obtained from healthy donors between 6 and 12 years old. All procedures were performed according to the protocol developed by Kerkis et al. [12]. The cells were cultivated until the fifth passage (P5, NestaCell™ product). The MSC phenotype of these cells was confirmed using the criteria defined by the International Society for Cellular Therapy (ISCT) [13, 15]. The hIDPSCs used in phase I clinical trial for HD were CD105-, CD73-,and CD90-positive and CD45-, CD34-, CD11b-, and HLA-DR-negative, as previously described by Kerkis et al. [12].

Case Rep Oncol 2022;15:413–422
DOI: 10.1159/000523896

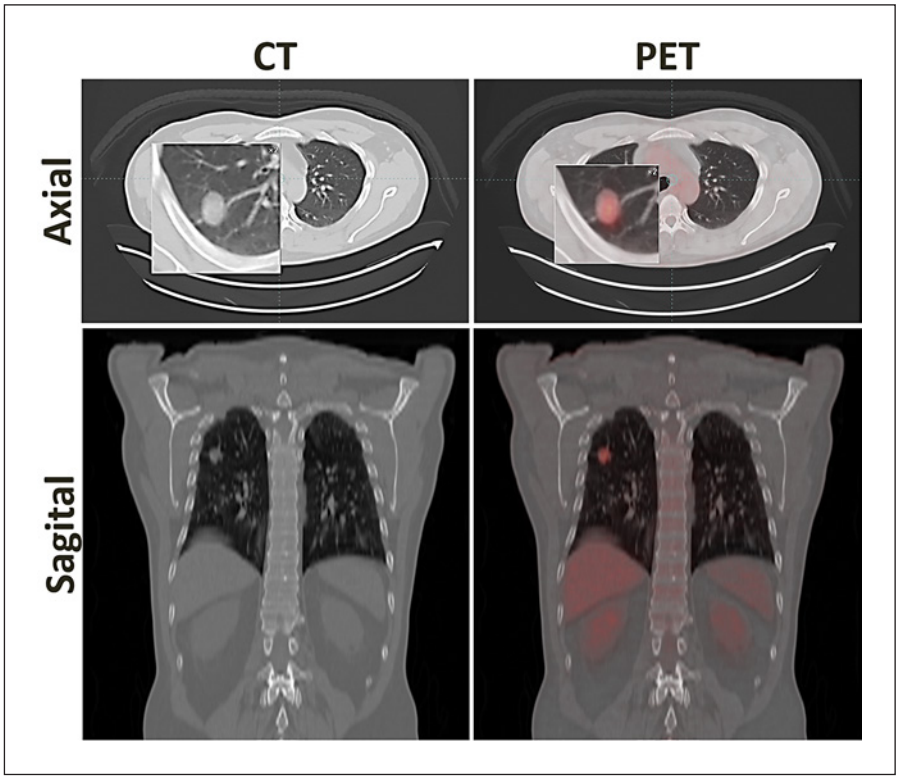

Fig. 2. CT and PET/CT showing the pulmonary nodule growth (verified in August 2020, after 2 years of the third hIDPSC IV infusion). PET/CT shows hypermetabolism compatible with granulomatous or neoplastic disease. PET/CT, positron electron tomography.

A new CT scan in January 2019 showed no change to the nodule dimensions (13 × 15 × 17 mm). The patient had a significant score reduction of the Unified Huntington's Disease Rating Scale (from 23 to 10 after the third infusion and 16 after 9 months after the third infusion).

The patient received a new hIDPSC on August 10, 2020. A new CTscan made per protocol in August 31, 2020, showed nodule enlargement (14 × 23 × 24 mm, Fig. 2). We reported this finding as a nonserious adverse event and referred the patient to an oncologist, who requested a positron electron tomography. It showed nodule hypermetabolism, compatible with granulomatous or neoplastic disease (Fig. 2). Both the oncologist and the pulmonologist requested bronchoscopy lung biopsy, which came positive for adenocarcinoma, predominantly papillary and moderately differentiated. A serious adverse event was reported to the IRB.

The patient underwent an upper right pulmonary lobectomy and lymphadenectomy by video-assisted thoracoscopic surgery and video-assisted mediastinoscopic lymphadenectomy in December 2020 at Vera Cruz Hospital (Campinas, Brazil). During the surgical procedure, the right superior pulmonary lobe was excised. The tumor specimen was dissected with the aid of a sterile scalpel to isolate the adenocarcinoma from the adjacent healthy tissue. A healthy lung tissue fragment adjacent to the neoplasm (sample 1) was collected and destined for RNA sequencing (RNA-seq). The neoplasm was sectioned into five pieces from edge to edge (samples 2–6). Tissue fragments were washed with sterile phosphate buffer saline (0.137 M NaCl, 0.0027 M KCl, 0.01 M Na2HPO4, and 0.0018 M KH2PO4, pH 7.4) and macerated

in 90 × 15 cm Petri dishes containing 1 mL of TRIzol reagent (Thermo Fisher Scientific, Carlsbad, CA, USA). Samples were collected and transferred to 1.5 mL polypropylene tubes. Each tube was identified from one to six according to the anatomical region of each piece. The tubes were transported on dry ice to the Genetics Laboratory of the Butantan Institute, where they were cryopreserved at −80°C. The total concentration of isolated RNA was obtained by the photometric method of UV-Vis at a wavelength of 260 nm, using NanoDrop 2000 (Thermo Fisher Scientific, Carlsbad, CA, USA). The quality (purity) of the RNA was verified by the values of the absorbance ratios A260/A230, where the values of A260/A230 different from the acceptable interval range of 2.0–2.2 indicate the presence of contaminants such as TRIzol. RNA quality was also confirmed using the BioAnalyzer 2100 instrument (Agilent, Carlsbad, CA, USA).

The isolated RNAs were sent to the CD Genomics facility (New York, NY, USA) for sequencing messenger RNA. For this, cDNA libraries were built from the isolated messenger RNAs. The cDNAs obtained were fragmented and ligated to adapters (RA5 – 5′-GTTCAGAGTTC-TACAGTCCGACGATC-3′ and RA3 – 5′-AGATCGGAAGAGCACACGTCT-3′). Using primers capable of annealing to these adapters, cDNAs were sequenced using the HiSeq 4000 platform; (Illumina, Carlsbad, CA, USA), generating 50 million reads of each sample. The sequencing files were exported and uploaded in the fast extension. Received files were analyzed using the Galaxy tool (available at https://usegalaxy.org/).

For this, initially, the quality of the sequenced bases was evaluated (QC – quality control). Such analysis was performed using the FastQC program (available at https://www.bioinformatics.babraham.ac.uk/projects/fastqc/). After confirming that the sequenced bases present acceptable levels of quality, the adapters were removed (i.e., trimmed) using the Cutadapt tool version 3.4 (available at https://cutadapt.readthedocs.io/en/stable/). To confirm that the removal of the adapter sequences happened accurately, the obtained sequences were subjected to an additional Q.C. step using the MultiQC tool (available at https://multiqc.info/). After this step, the sequences were aligned using the STAR aligner (available at https://www.biostars.org/p/428681/), using as a reference the transcript GRCh37, obtained from the reference human genome (available at https://www.gencodegenes.org/human/release_36lift37.html). The identified transcripts were normalized and counted using the HT-Seq tool (available at https://docs.gdc.cancer.gov/Encyclopedia/pages/HTSeq-Counts/).

In order to assess the possible presence of CTIPDh (NestaCell™), the transcriptomes of the six different fragments were obtained from the neoplasm and compared to the transcriptome of the hIDPSC (NestaCell™). For this, two different statistical approaches were used: (i) principal component analysis (PCA) and (ii) differential expression using the NOIseq tool.

PCA is a mathematical method widely used in exploratory data analysis [16]. This method is based on the orthogonal conversion of gene expression values obtained from a dataset of a sample into values of linearly correlated variables – principal component [17]. This conversion allows reducing the dimensionality of data sets, facilitating interpretation in order to reduce the loss of information [17]. In this way, the PCA provides distance maps between samples that allow comparing the transcriptomic of multiple samples simultaneously [17]. NOIseq is a robust method that allows evaluating differential gene expression from RNA-seq data (number of normalized reads) [18, 19].

Postsurgical histology showed well-differentiated invasive adenocarcinoma infiltrating lung parenchyma (16 × 12 mm) without angiolymphatic invasion, pleural surgical margin free of neoplasia, absence of metastases in hilar, mediastinal, and subcarinal lymph nodes. Immunohistochemistry showed that the neoplasm was primary lung (CK7-, TTF1-, and naps in A-positive and CK20-negative).

Case Rep Oncol 2022;15:413–422
DOI: 10.1159/000523896

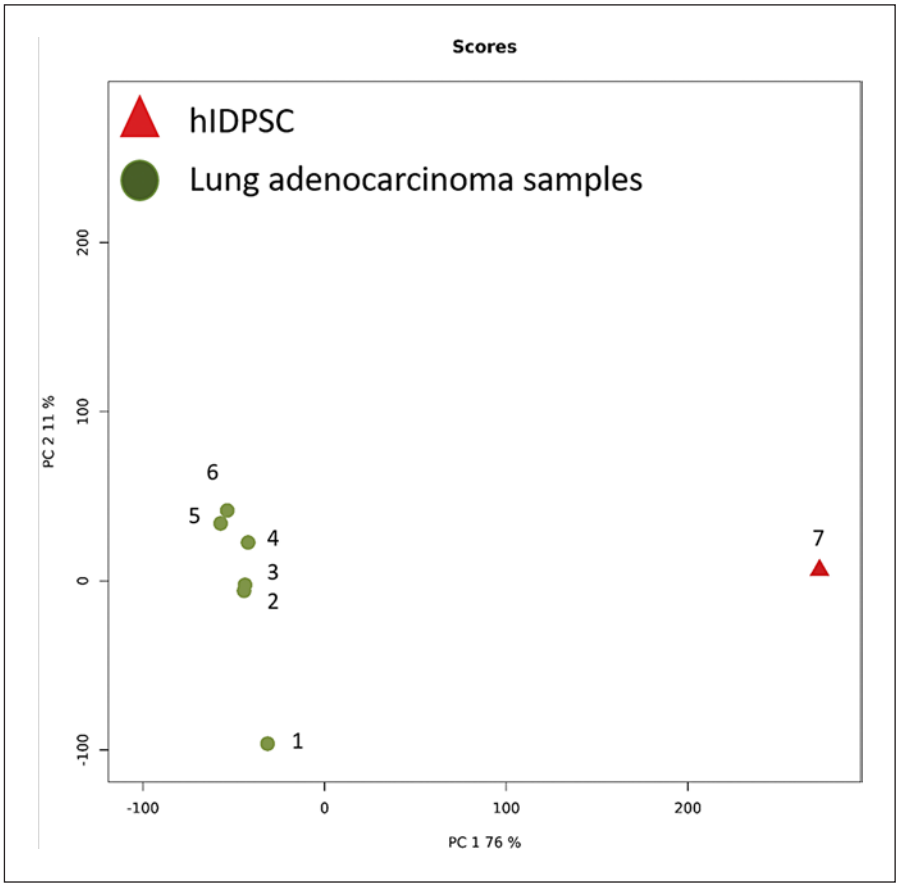

Fig. 3. PCA results showing the linear distance of the main component of hIDPSCs in relation to the main enrolled in the clinical trial. Greater distance from fragment 1 (collected from an area adjacent to the neoplasm margin), as well as the greater distance from fragment 4 (tumor core) in relation to fragments 2/3 and 5/6 (distally located in relation to the tumor core). This result reflects intra-tumoral heterogeneity.

We assessed the possible presence of hIDPSCs within this lung adenocarcinoma. The gene expression values obtained from six neoplasm sampling regions were orthogonally converted into six principal component values.

These values were linearly correlated with the main component from the patient's gene expression of transplanted hIDPSCs. In addition, the results of PCA showed a linear distance between the adenocarcinoma (samples 2–6) and lung tissue fragments adjacent to the lung cancer (sample 1, Fig. 3). This indicates that these samples' main components have a transcriptional profile different from other tumor areas, as expected. Results also showed that sample 4, obtained from the tumor core, was linearly distant from samples 2/3 and 5/6, all near the tumor edge (Fig. 3). This shows the tumor edge-to-core heterogeneity. However, the PCA results also showed a significant linear distance between the adenocarcinoma (samples 2–6), the healthy lung tissue (sample 1), and the hIDPSCs (sample 7, Fig. 3), suggesting the absence of hIDPSCs within the tumor tissue. Confirming these results, we performed a differential expression analysis based on the count of transcripts' normalized reads of each sample (NOIseq). Most transcripts of the hIDPSCs are not found in the adenocarcinoma transcriptome (Fig. 4).

The patient was discontinued from the clinical trial, and the adverse event followed according to GCP. He remained asymptomatic after 6 months of follow-up. The surgery was considered curative for the neoplasms stage (Fig. 5).

Case Rep Oncol 2022;15:413–422
DOI: 10.1159/000523896

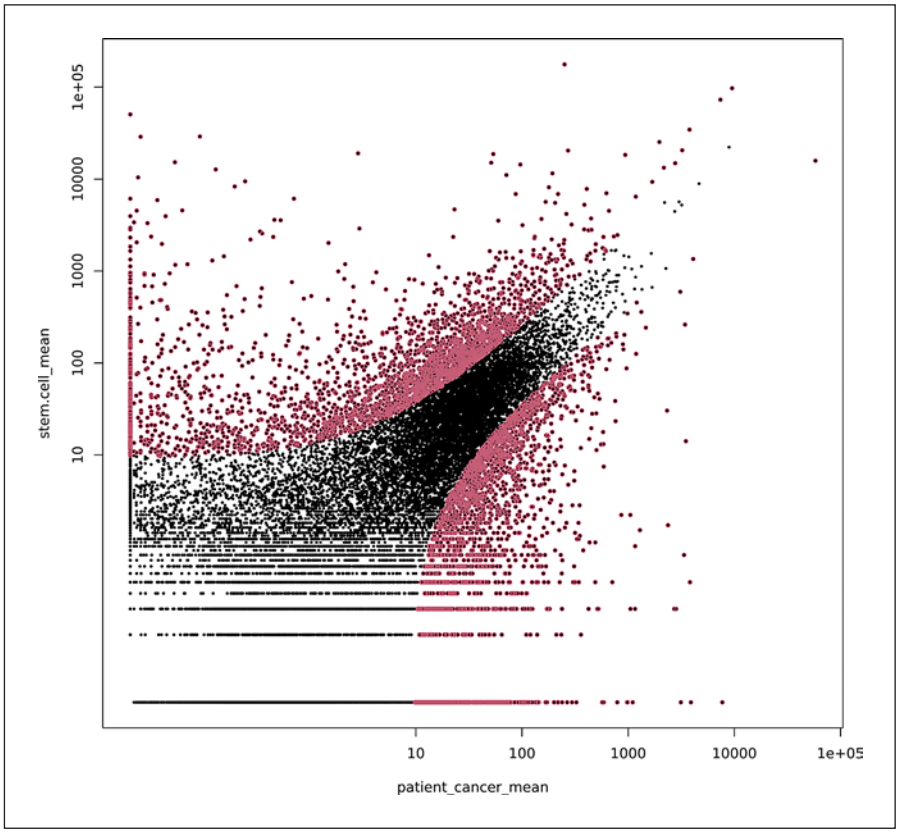

Fig. 4. Differential expression analysis (nonparametric) by NOIseq showing that genes overexpressed in hIDPSCs are not expressed in lung adenocarcinoma fragments. Red dots indicate differentially expressed genes, and black dots, genes commonly expressed across samples.

Discussion

To our knowledge, this is the first report of MSCs administration in a patient with preexisting cancer. We investigated the presence of hIDPSCs (NestaCell™) in the lung adenocarcinoma of a patient enrolled in a clinical trial. We performed the RNA-seq neoplasm samples and compared the tumoral and hIDPSCs transcriptomes using two statistical approaches: PCA and NOIseq. Our data suggest that, although IV cell infusion facilitates the MSCs trap into the lung, due to the pulmonary first-pass, the hIDPSCs administrated IV did not show long-term tropism or homing for the lung adenocarcinoma.

As expected, the PCA showed a linear distance between the lung adenocarcinoma (samples 2–6) and heath lung tissue nearby the neoplasm (sample 1, Fig. 3), confirming that the main component of the lung adenocarcinoma is different from the healthy lung. The PCA also showed a linear distance between the lung adenocarcinoma samples (Fig. 3), which shows spatial tumor heterogeneity, as reported by other authors by single-cell RNA-seq [20–22]. We observed a significant linear distance between the lung adenocarcinoma to the hIDPSCs (Fig. 3), confirmed by the NOIseq analysis (Fig. 4). We also did not detect the presence of hIDPSCs (NestaCell™) in the healthy lung tissue nor within the five adenocarcinoma samples.

TME produces and secretes proinflammatory cytokines and chemokines [23], which can recruit endogenous MSCs within the TME. Once into the TM, these cells can suppress the antitumor immune response [24]. For this reason, there is a rising concern on the

Case Rep Oncol 2022;15:413–422
DOI: 10.1159/000523896

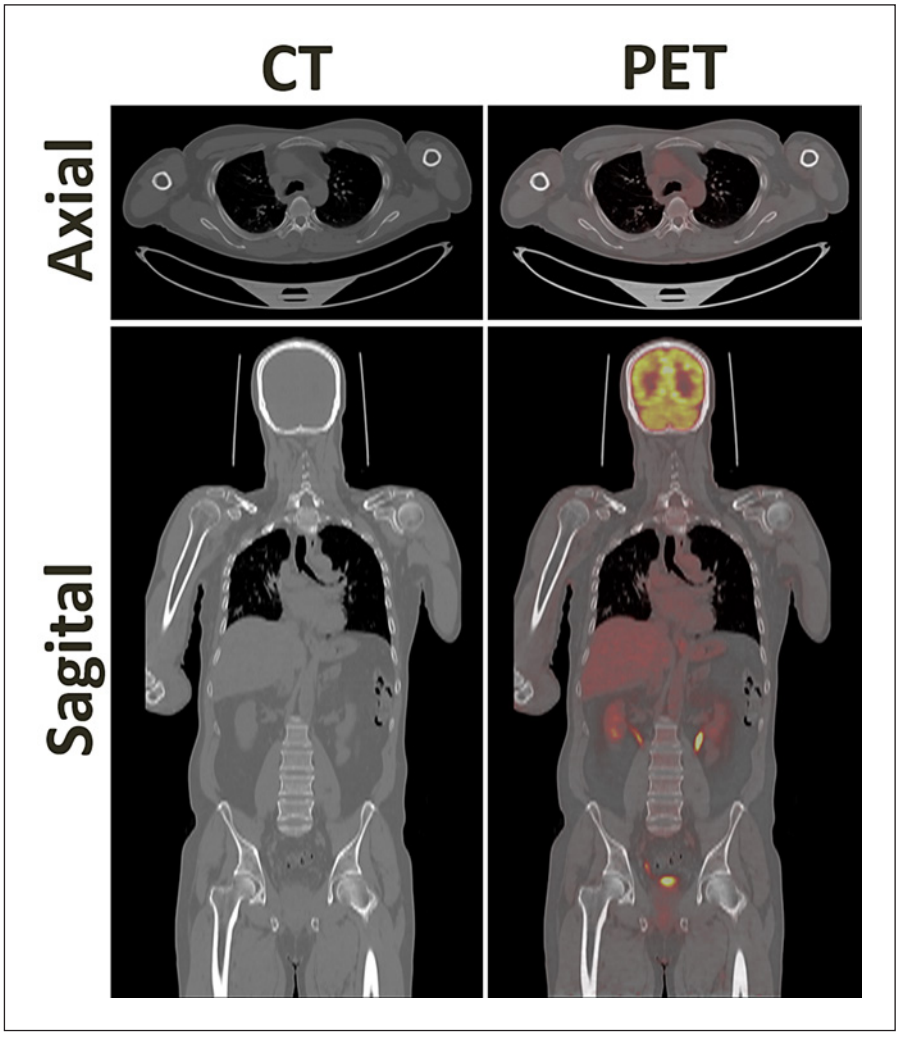

Fig. 5. CT and PET/CT performed in July 2021 as part of the follow-up of the patient showing no cancer recurrence or metastasis after the surgical treatment. PET/CT, positron electron tomography.

safety of MSC-based therapy in patients susceptible to malignancies or having preexisting cancer [24]. Despite this concern, there is no evidence in humans that MSC-based therapy can contribute to cancer development, progression, or metastasis.

Conclusion

This report suggests that hIDPSCs neither homed nor grafted into a preexisting primary lung adenocarcinoma.

Statement of Ethics

Written informed consent was obtained from the patient for publication of this case report and any accompanying images. The clinical protocol, informed consent form, and all other applicable documents were submitted to the Research Ethics Committees of the

research center, which reviewed and approved the trial according to current legislation (CEP/CONEP 3.826.751). The study was conducted according to the good clinical practices (clinicaltrials.gov identifier NCT02728115).

Conflict of Interest Statement

The authors have no conflict of interest to declare.

Funding Sources

The authors thank for Cellavita Pesquisas Científicas Ltda., and Butantan Institute/Foundation by the financial support. The funders had no role in study design, data collection and analysis, decision to publish, or preparation of the manuscript.

Author Contributions

Joyce Macedo da Silva, Rodrigo Pinheiro Araldi, and Irina Kerkis contributed with study design and development, and data analysis and wrote the manuscript. Joyce Macedo da Silva provided patient samples and interpreted data. Joyce Macedo da Silva, Rodrigo Pinheiro Araldi, and Cristiane Wenceslau Valverde conducted experiments, acquired, and analyzed the data. Gabriel Avelar Colloza-Gama conducted bioinformatics analysis. Rodrigo Pinheiro Araldi was responsible for the RNA-seq. Irina Kerkis supervised research. Eduardo Pagani and Ariye Sid reviewed and edited the manuscript.

Data Availability Statement

All data generated or analyzed during this study are included in this article. Further inquiries can be directed to the corresponding authors.

References

1 Hong EP, MacDonald ME, Wheeler VC, Jones L, Holmans P, Orth M, et al. Huntington's disease pathogenesis: two sequential components. J Huntingtons Dis. 2021 Feb;10(1):35–51.
2 Haddad MS, Wenceslau CV, Pompeia C, Kerkis I. Cell-based technologies for Huntington's disease. Dement Neuropsychol. 2016 Dec;10(4):287–95.
3 Pritchard A, Tousif S, Wang Y, Hough K, Khan S, Strenkowski J, et al. Lung tumor cell-derived exosomes promote M2 macrophage polarization. Cells. 2020 May;9(5):1303.
4 Eskandari N, Boroujeni ME, Abdollahifar MA, Piryaei A, Khodagholi F, Mirbehbahani SH, et al. Transplantation of human dental pulp stem cells compensates for striatal atrophy and modulates neuro-inflammation in 3-nitropropionic acid rat model of Huntington's disease. Neurosci Res. 2021 Sep;170:133–44.
5 Luzuriaga J, Polo Y, Pastor-Alonso O, Pardo-Rodríguez B, Larrañaga A, Unda F, et al. Advances and perspectives in dental pulp stem cell based neuroregeneration therapies. Int J Mol Sci. 2021;22(7):3546.
6 da Costa VR, Araldi RP, Vigerelli H, D'Ámelio F, Mendes TB, Gonzaga V, et al. Exosomes in the tumor microenvironment: from biology to clinical applications. Cells. 2021;10(10):2617.
7 Hayat H, Hayat H, Dwan BF, Gudi M, Bishop JO, Wang P. A concise review: the role of stem cells in cancer progression and therapy. Onco Targets Ther. 2021 Apr;14:2761–72.
8 Hardy WR, Moldovan NI, Moldovan L, Livak KJ, Datta K, Goswami C, et al. Transcriptional networks in single perivascular cells sorted from human adipose tissue reveal a hierarchy of mesenchymal stem cells. Stem Cells. 2017 May;35(5):1273–89.

9 Hill BS, Pelagalli A, Passaro N, Zannetti A. Tumor-educated mesenchymal stem cells promote pro-metastatic phenotype. Oncotarget. 2017 Sep;8(42):73296–311.
10 Kumari D. States of pluripotency: naïve and primed pluripotent stem cells. Pluripotent stem cells – from the bench to the clinic. InTechOpen; 2016.
11 Sai B, Dai Y, Fan S, Wang F, Wang L, Li Z, et al. Cancer-educated mesenchymal stem cells promote the survival of cancer cells at primary and distant metastatic sites via the expansion of bone marrow-derived-PMN-MDSCs. Cell Death Dis. 2019 Dec;10(12):941.
12 Kerkis I, Kerkis A, Dozortsev D, Stukart-Parsons GC, Gomes Massironi SM, Pereira LV, et al. Isolation and characterization of a population of immature dental pulp stem cells expressing OCT-4 and other embryonic stem cell markers. Cells Tissues Organs. 2006;184(3–4):105–16.
13 Dominici M, Le Blanc K, Mueller I, Slaper-Cortenbach I, Marini F, Krause D, et al. Minimal criteria for defining multipotent mesenchymal stromal cells. The International Society for cellular therapy position statement. Cytotherapy. 2006 Jan;8(4):315–7.
14 Macedo J, Pagani E, Wenceslau C, Ferrara L, Kerkis I. A pahse I clinical trial on intravenous administration of immature human dental pulp stem cells (NestaCell) to Huntington's disease patients. Cytotherapy. 2021 Apr; 23(4):1.
15 Galipeau J, Krampera M, Barrett J, Dazzi F, Deans RJ, DeBruijn J, et al. International Society for cellular therapy perspective on immune functional assays for mesenchymal stromal cells as potency release criterion for advanced phase clinical trials. Cytotherapy. 2016 Feb;18(2):151–9.
16 Son K, Yu S, Shin W, Han K, Kang K. A simple guideline to assess the characteristics of RNA-seq data. Biomed Res Int. 2018 Nov;2018:2906292.
17 Jolliffe IT, Cadima J. Principal component analysis: a review and recent developments. Philos Trans A Math Phys Eng Sci. 2016 Apr;374(2065):20150202.
18 Tarazona S, García F, Ferrer A, Dopazo J, Conesa A. NOIseq: a RNA-seq differential expression method robust for sequencing depth biases. EMBnet J. 2012 Feb;17:18.
19 Tarazona S, Furió-Tarí P, Turrà D, Pietro AD, Nueda MJ, Ferrer A, et al. Data quality aware analysis of differential expression in RNA-seq with NOISeq R/bioc package. Nucleic Acids Res. 2015 Jul;43(21):e140.
20 Suo S, Cheng J, Cao M, Lu Q, Yin Y, Xu J, et al. Assessment of heterogeneity difference between edge and core by using texture analysis. Acad Radiol. 2016 Sep;23(9):1115–22.
21 Wang Y, Li X, Peng S, Hu H, Wang Y, Shao M, et al. Single-cell analysis reveals spatial heterogeneity of immune cells in lung adenocarcinoma. Front Cell Dev Biol. 2021 Aug;9:638374.
22 Xing X, Yang F, Huang Q, Guo H, Li J, Qiu M, et al. Decoding the multicellular ecosystem of lung adenocarcinoma manifested as pulmonary subsolid nodules by single-cell RNA sequencing. Sci Adv. 2021 Jan;7(5):eabd9738.
23 O'Callaghan DS, O'Donnell D, O'Connell F, O'Byrne KJ. The role of inflammation in the pathogenesis of non-small cell lung cancer. J Thorac Oncol. 2010;5(12):2024–36.
24 Gazdic M, Simovic Markovic B, Jovicic N, Misirkic-Marjanovic M, Djonov V, Jakovljevic V, et al. Mesenchymal stem cells promote metastasis of lung cancer cells by downregulating systemic antitumor immuner response. Stem Cells Int. 2017;2017:6294717.